Progress In Electromagnetics Research M, Vol. 104, 1–12, 2021

A Multidirectional Triple-Band Rectenna for Outdoor RF Energy Harvesting from GSM900/GSM1800/UMTS2100 toward Self-Powered IoT Devices

Minh Thuy Le*, Quang Chung Tran, Anh Tuan Le, and Dinh Minh

Abstract—Due to low power density, it is difficult for a single-band rectenna to harvest enough power for IoT devices like wireless sensors. Thus to supply these consuming devices, harvesting RF energy from multiple frequencies is a solution to enhance the amount of harvested DC power. In this work, we introduce a triple-band rectenna, working at 900 MHz, 1.8 GHz, and 2.1 GHz, three readily available bands in the ambience, for energy harvesting application. The proposed rectenna consists of three monoband rectifiers connected to a multi-band receiving antenna via a highly efficient triplexer. The antenna is made by superposing two concentric rings and manipulating their radii to achieve the desirable operating frequencies, with antenna gains of respectively 2.5 dBi, 4.5 dBi, and 4 dBi. The contiguous triplexer is made by connecting open stubs band-reject filters and optimizing their positions, resulting in the triplexing efficiency higher than 75%. The measured RF-DC efficiency under −10 dBm triple-tone input power is 40%.

1. INTRODUCTION

The rapid development of low-powered IoT devices comes with the demand for a reliable power supply. Traditionally, most electronic devices use batteries, which have limited lifespan, as their primary power source. Toward a sustainable operation, the battery has to be replaced by, or at least supported with, other more sustainable sources. RF energy harvesting emerges as a solution due to its all-day availability, ubiquity, and stability. Despite that potential, the very low power density of available ambient RF sources is the reason hindering the applicability of this solution. Although some low-powered IoT devices only consume several nanowatts in their sleep mode and several dozen milliwatts in their active mode [1–3], that most RF sources available in the ambient environment yield less than $1\,\mu W/cm^2$ power density [4, 5] makes it almost impossible for RF waves to sustain any device in their active mode. For instance, the wireless sensors in [2] consume up to 23.7 mW while the sensors in [3] consume 11 mW.

To deal with the problem, one solution of is to use multiband rectenna to collect power from multiple frequency bands. Several works have been dedicated to that. For example, in [6], the dual-band rectenna achieves an RF-DC conversion efficiency of 26% and 15% at 2.45 GHz and 3.6 GHz under −10 dBm input power, respectively, while in [7], also under −10 dBm input power, the triple-band rectenna yields a conversion efficiency of 41%, 30%, and 25% at 0.9 GHz, 1.8 GHz, and 2.1 GHz. It is notable, however, that most of earlier multiband rectennas follow the same pattern of employing a single multiband/wideband rectifier. This method, although achieves compactness, is difficult to execute due to several reasons. First, matching the input impedance of the rectifier at different frequencies is

Received 13 June 2021, Accepted 14 July 2021, Scheduled 28 July 2021
* Corresponding author: Minh Thuy Le (thuy.leminh@hust.edu.vn).
The authors are with the Department of Instrumentation and Industrial Informatics, School of Electrical Engineering, Hanoi University of Science and Technology, 1st Dai Co Viet, Hanoi, Vietnam.

not an easy task. More often than not, the impedance is matched at one frequency and strikingly mismatched at others. Second, as shown in Fig. 1 and other surveys [5], each frequency band has a different power density compared to others while the rectenna's efficiency, due to the nonlinearity of the diodes, depends heavily on the input power. Therefore, to achieve optimal performance at each frequency simultaneously is still a difficult task. Finally, even if a wideband rectifier can be created, high efficiency at low input power still cannot be guaranteed because of the multi-stage matching circuit [8, 9]. To counter this issue, one may use monoband rectifiers, which are considerably simpler and less lossy, in conjunction with a multiplexer circuit. However, in this case, loss occurs largely on the multiplexer. Earlier multiplexers have complicated structures [10], thus result in higher losses. Some even employ discontinuous transmission lines, placing gaps in the propagating direction of the signals or using lumped components like capacitors or inductors [10–12] resulting in even higher losses.

Another difficulty is in the design of the antenna. Because the positions of the RF sources are usually unknown, a common requirement for energy harvesting antennas is the omnidirectional or multidirectional radiation pattern. Many earlier works employ complex geometry to accomplish this task. For example, in [13–16], antennas are designed with Hilbert fractal geometry, resulting in wide bandwidths and either omnidirectionality or multi-directionality. In [17], the fractal geometry with triangular shapes also leads to multiple operating bands. The expandability, the ability to incorporate more frequency bands, is also limited.

To overcome the above difficulties, in this work, we propose a simple triple-band rectenna based on three monoband rectifiers operating at three distinct frequencies, connected to a multiband receiving antenna via an efficient triplexer. By employing monoband rectifiers, which are undoubtedly easier to create, this triple-band rectenna configuration helps reduce the complexity significantly. The triplexer is made with simplicity, employing no lumped component and with continuous lines. Therefore, the triplexer produces better efficiency. It can also be expanded into a quadruplexer or more via simple modifications. The antenna also yields a simple structure with only two circular rings attached to each other. It can also be modified to have more resonant frequencies by simply adding more rings. The expandability is thus another advantage of this rectenna.

The rectenna is intended to operate as the power supply of low-powered IoT devices for environmental monitoring, such as wireless sensors nodes. Therefore, it must harvest the most suitable bands for outdoor operation. Our goal is to replace the unsustainable battery in IoT devices with a cleaner power supply. If this goal is still too far to achieve, then at least, the triple-band rectenna may sustain the consuming IoT devices in sleep mode or some limited modes. In addition, they may prolong the battery lifetime if being used simultaneously with the battery, making it runs out more slowly.

This paper is arranged as follows. Section 2 is the design of the rectenna, consisting of an antenna, a triplexer, and rectifiers. Section 3 examines the rectenna's performance, and finally, Section 4 is the conclusion.

2. RECTENNA DESIGN

2.1. Outdoor RF Power Density Measurement

Before designing the rectenna, we measured the power density of these four bands in the ambience to determine the input power levels. The 900 MHz, 1.8 GHz, and 2.1 GHz bands were measured outdoor at the campus of the university, close to a base station tower while the Wi-Fi is available indoor, using a Keysight N9937A handheld spectrum analyser (Fig. 1(a)). The result is shown in Fig. 1(b).

According to our survey result, in the ambience, there are four dominating RF frequencies to harvest: the GSM900, GSM1800, UMTS2100, and ISM2400. There are also many lower frequency bands such as television, amplitude-modulated (AM), and frequency-modulated (FM) signals. However, these frequencies are too low, resulting in a very bulky system, unsuitable in practical applications. For instance, a half-wavelength dipole antenna, working at the very-high-frequency (VHF) AM band around 50 MHz, will have a length of 3 meters, which is obviously not a good choice for small, compact applications like IoT devices. Among the four aforementioned bands, the 2.4 GHz band is unstable. In fact, as we have observed during the RF spectra measurement, Wi-Fi signals are intermittent, only arrive in a short period of time before disappearing. Wi-Fi is also predominantly indoor, which is the main reason that it is unsuitable for this outdoor rectenna. Therefore, 900 MHz, 1.8 GHz, and 2.1 GHz

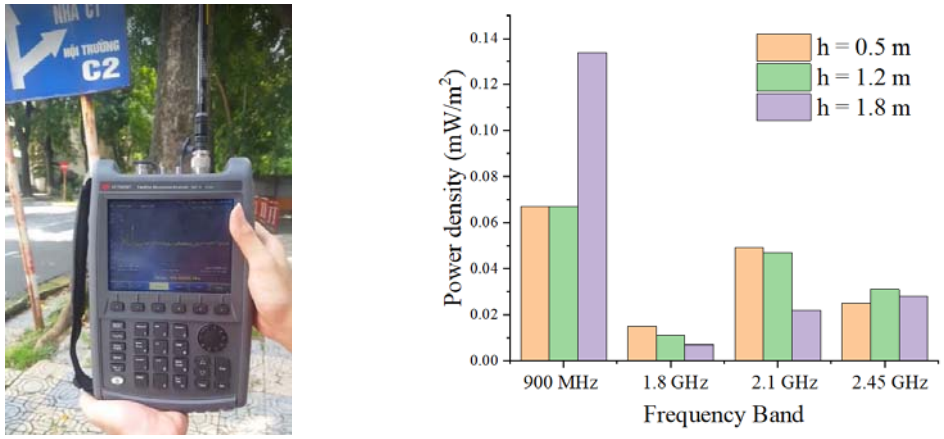

(a) (b)

Figure 1. (a) The measurement of RF power density at HUST campus; (b) the measured power densities of the four RF bands: 900 MHz, 1.8 GHz, 2.1 GHz, and 2.45 GHz.

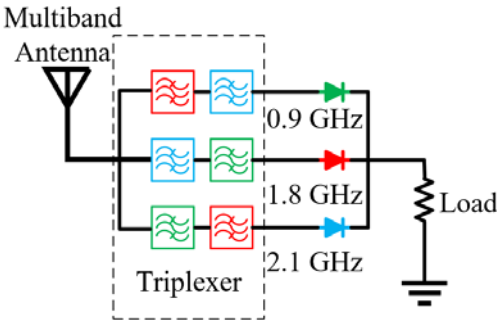

Figure 2. Configuration of the triplexer-based triple-band rectenna.

are more suitable for energy harvesting due to their stability and availability. The GSM900 band yields the highest power density, making it the primary source while the other two act as supplementary bands. The band of 2.6 GHz is not yet available in the environment in our place right now, and it will be used soon for New Radio (5G).

The block diagram of the proposed triple-band rectenna is shown in Fig. 2. The multiband antenna receives incident RF waves, then transfer them to the triplexer. This triplexer splits the power stream into three distinct frequencies and delivers them to the corresponding rectifier. The triplexer consists of three parallel channels, and each is made by two band-reject filters.

2.2. Multiband Antenna Design

2.2.1. Antenna Analysis

As mentioned in the previous part, for energy harvesting, omnidirectional or multi-directional antennas are the most suitable since the locations of sources are often uninformed. The only weakness of omnidirectional antennas is their low gains, thus low received power. However, this problem can be readily addressed by harvesting multiple bands.

The design of the multiband monopole antenna is shown in Fig. 3. The antenna is made by superposing two rings together on a 0.8 mm-thick RO4003C substrate (dielectric constant $\varepsilon = 3.55$, loss tangent $\tan\delta = 0.0027$). A finite ground is placed at the opposite side of the substrate.

The initial design is a single-ring antenna with a radius of 24 mm, and the height of the ground plane and feed length are arbitrarily chosen as 11 mm. The single-ring antenna is simulated using CST

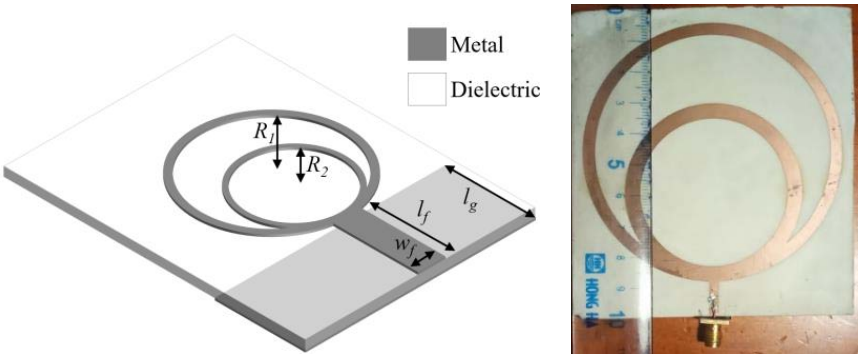

Figure 3. The design and photo of the proposed multiband antenna.

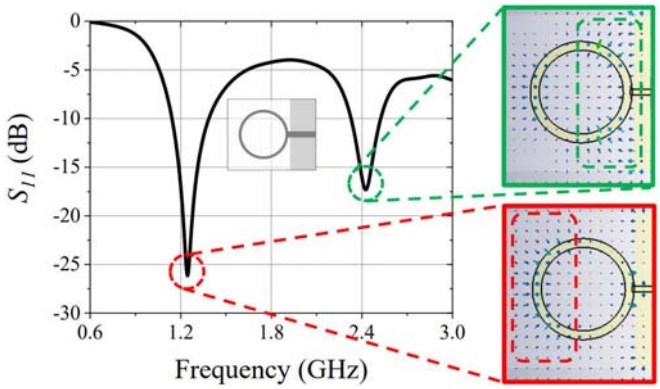

Figure 4. Simulated S_{11} of the single-ring monopole antenna and the electric-field distribution at two resonant frequencies.

Studio Suite. The simulated S_{11} shown in Fig. 4 exhibits two resonant frequencies at 1.25 GHz and 2.4 GHz. At the first resonant frequency, the electric field is located mostly at the upper edge of the ring (marked by the red dashed box) and at the ground like in normal monopole antennas. The first resonance frequency therefore depends on the length of the antenna (the ring's diameter plus the length of the feed line). At the second frequency, in addition to the upper edge and the ground, the electric field is also strong at the two lower sides of the ring (marked by the green dashed box). Therefore, the second frequency also depends on the antenna's width (the ring's diameter). The two frequencies can thus be independently tuned by changing the feed's length and ring diameter.

The second ring is added forming the proposed antenna as in Fig. 3. As we mentioned above, each ring's diameter is determined corresponding to two resonant frequencies. Meanwhile, the distance from the ground to the centre of each ring corresponds to its first resonance frequency. By tuning the diameters of both rings, we can obtain the desired resonant frequencies. The method of overlapping resonators with different resonant frequencies is also employed in by Pandey et al. [18], in which multiple triangles are superposed to create a wideband monopole antenna.

From the presented analysis, the two-ring monopole antenna is designed as follows: The bigger ring has its radius and feed length tuned to achieve the 900 MHz and 2.1 GHz resonant frequencies. To create the third resonant frequency, another smaller ring is added, and the mutual coupling between two rings will be considered. This ring is tuned to resonate at 1.8 GHz and 2.6 GHz. The final dimensional parameters are $R_1 = 42$ mm, $R_2 = 29$ mm, $w_f = 3$ mm, $l_f = 11$ mm, and $l_g = 11$ mm.

2.2.2. Antenna Simulation and Measurement Results

The double-ring antenna is simulated using CST Studio Suite. The simulated and measured S_{11} of the multiband two-ring antenna are shown in Fig. 5. The antenna possesses four resonant frequencies

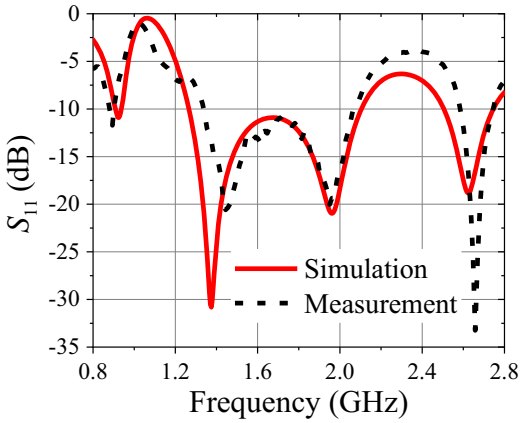

Figure 5. The simulated and measured S_{11} of the multiband antenna.

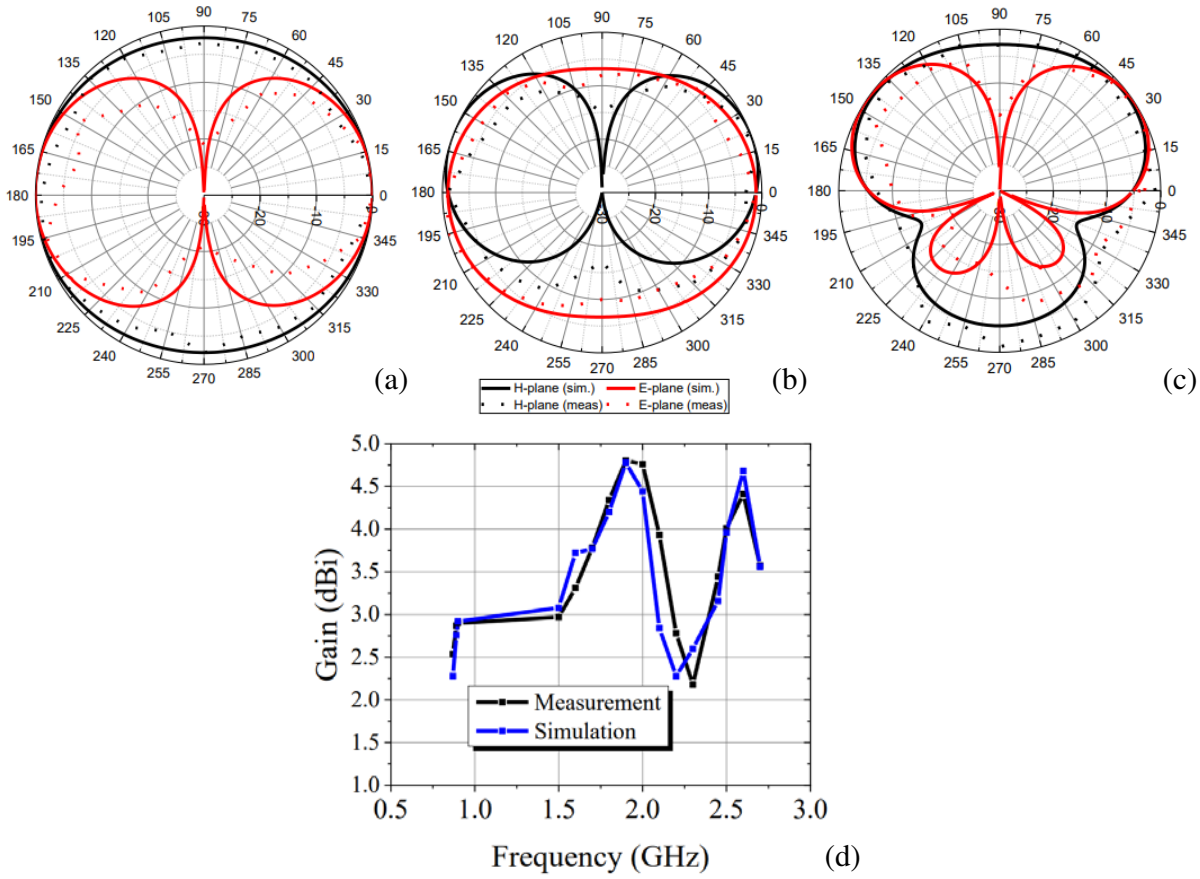

Figure 6. The normalized radiation pattern at (a) 900 MHz, (b) 1.8 GHz, and (c) 2.1 GHz, and (d) the peak gain at different frequencies.

at 900 MHz, 1.5 GHz, 2 GHz, and 2.7 GHz, with a wide resonant bandwidth spanning from 1.4 GHz to 2.15 GHz. The two higher frequencies are shifted from the single-ring cases due to the rings' mutual coupling, but the three desired frequencies still stay inside the −10 dB bandwidth. The antenna's radiation pattern is displayed in Fig. 6. In general, the pattern is omnidirectional at 900 MHz and 1.8 GHz. At 2.1 GHz, the pattern is near-omnidirectional. It has two lower dips at 200° at 340°, but

outside of those dips, the gain is still very stable. The peak gain at 900 MHz, 1.8 GHz, and 2.1 GHz are respectively 2.5 dBi, 4.8 dBi, and 4 dBi. As mentioned above, the 2.6 GHz source is not available yet in the environment, thus in this rectenna design, this frequency is not considered.

2.3. Triplexer Design

Quarter-wavelength open stubs are able to operate as band-reject filters. As a proof for this, we consider the case of an open stub of length l and characteristic impedance Z_o. It is connected to input port 1 and output port 2. For simplicity, we let the impedances of these ports be Z_o as well. The input impedance of the stub Z_1 is expressed as follows:

$$Z_1 = -iZ_o \cot(\beta l) \tag{1}$$

where i is the imaginary unit, $\beta = 2\pi/\lambda$ the wave number, $\lambda = c/f$ the wavelength at frequency f, and c the wave propagation velocity. Because the stub is parallel to the output port 2, the impedance Z_2 seen from the input port 1 is therefore:

$$Z_2 = \frac{Z_1 Z_o}{Z_1 + Z_o} = \frac{iZ_o \cot(\beta l)}{i\cot(\beta l) - 1} \tag{2}$$

The reflection coefficient Γ at the input port 1 is therefore:

$$\Gamma = \frac{Z_2 - Z_o}{Z_2 + Z_o} = \frac{-i}{2\cot(\beta l) - 1} \tag{3}$$

For $l = \lambda/4$, $\cot(\beta l) = \cot(\pi/4)$ reaches zero, and Γ reaches unity, leading to total reflection. The frequency f is thus rejected, and the stub becomes a band-reject filter.

The triplexer is also fabricated on a 0.8 mm-thick RO4003C substrate. The image of the triplexer is shown in Fig. 7. The band-reject filters are made by quarter-wavelength open stubs, which are bent to reduce size.

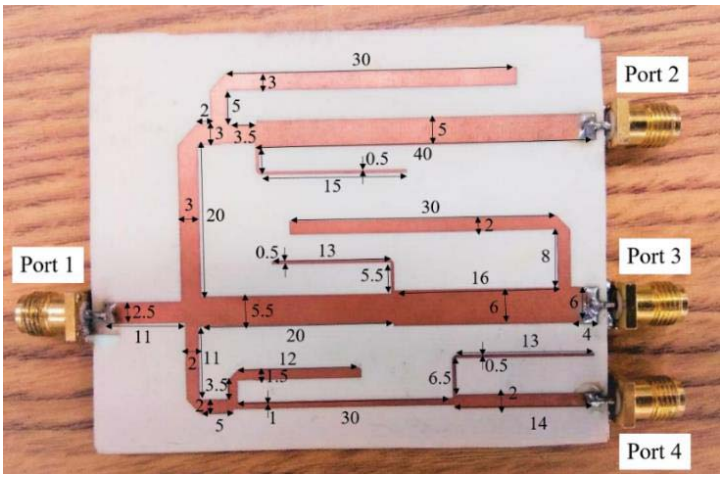

Figure 7. Actual image and parameters of the triplexer. Port 1 is the input port, Port 2, 3, 4 are the three output ports corresponding to 2.1 GHz, 1.8 GHz, and 900 MHz, respectively. The dimensions are in mm.

The triplexer is designed using numerical optimization in the Advanced Design Software (Keysight ADS). The optimization of each passband is carried out, then they are replaced by equivalent impedances when the 1-to-3 power divider is designed separately to reduce the complexity. The simulated and measured S-parameters of the triplexer are displayed in Fig. 8. The insertion loss at 900 MHz, 1.8 GHz, and 2.1 GHz are respectively 0.36 dB, 1.15 dB, and 0.73 dB, corresponding to 92%, 75%, and 82% transmission efficiencies. This performance is higher than most previously introduced triplexers or

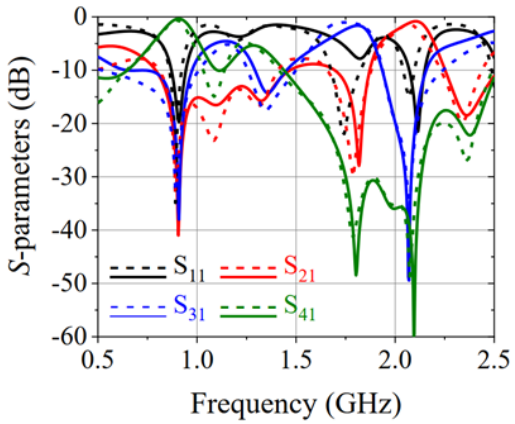

Figure 8. Simulated and measured S-parameters of the triplexer, the solid lines are simulation results, the dashed lines are measurement results.

Table 1. A comparison between the proposed triplexer and related works.

Work	Frequency (GHz)	Efficiency (%)
[10]	2.5, 2.8, 3.5	66, 58, 63
[11]	3.4, 3.9, 4.6	63, 63, 63
[12]	1.5, 2.2, 3	51, 59, 63
[19]	1.5, 1.75, 2	46, 44, 43
[20]	1.8, 2.1, 2.6	74, 59, 48
This work	0.9, 1.8, 2.1	92, 75, 82

multiplexers in general, as shown in Table 1. The proposed triplexer uses a simpler structure. Instead of band-pass filters, band-reject filters are employed. The propagating direction is continuous, and no lumped component appears. The structure is also considerably simpler, resulting in the better performance.

2.4. Rectifiers' Design

Three voltage-doubling rectifiers are designed and fabricated on a 0.8 mm-thick RO4003C substrate. The SMS7630 Schottky diode is employed due to its good performance at low input power [21].

A key advantage of the employed configuration compared to the multiband rectifiers is the simplicity in rectifier design. Unlike monoband rectifier, multiband rectifiers usually employ multi-stage matching circuit, with a lot of lumped components, multiple matching stubs, and long transmission lines [6–9, 22–24]. This makes multiband rectifiers difficult to design and yield high loss on the matching circuits. Instead of building a multi-stage matching circuit, each rectifier only has to match its impedance with 50 Ω at one narrow band around one single frequency. Another disadvantage of a multiband rectifier is that it requires a complicated multiband filter to efficiently remove all residual harmonics, while a radial stub or a shunted capacitor is enough for monoband rectifier.

The schematics and images of the three rectifiers are displayed in Fig. 9 and Fig. 10. The design procedure of each rectifier is as follows: First, the radial stub, which operates as a harmonic filter is designed. Its radius and angle are optimized to block the corresponding frequency and its odd harmonics. The 900 MHz and 1.8 GHz use an addition 470 pF capacitor to reject the AC harmonics, in conjunction with the radial stub, because in simulation, the residual harmonic of these rectifiers is relatively high. Then the diodes, capacitors, and harmonic filter are linked together. Their input impedance Z' is measured in the simulation tool. Then it is matched with 50 Ω using the matching

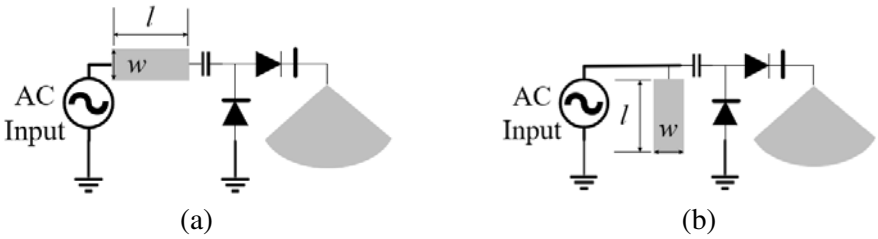

Figure 9. The schematic of (a) the 1.8 GHz and 2.1 GHz rectifiers, and (b) the 900 MHz rectifier.

Figure 10. Actual images of three single-band rectifiers.

circuit. For 1.8 GHz and 2.1 GHz, the matching circuit is only a transmission line of length l, width w, characteristic impedance Z_o depending on w, electrical length θ depending on l and the frequency. The impedance after matching Z is expressed as:

$$Z = Z_o \frac{Z_o + iZ' \tan(\theta)}{Z' + iZ_o \tan(\theta)} \tag{4}$$

Z_o and θ are then determined in order to obtain $Z = 50\,\Omega$ at the desired frequency. Then by using well-known formulas in [25], find the suitable values for l and w.

The width and length of this transmission line are optimized to achieve a $50\,\Omega$ input impedance at the corresponding frequency. For the 900 MHz, due to the low frequency, the size of the matching circuit will be large if only one transmission line is employed; therefore, an open stub is added, with an input impedance of Z_1. The matched impedance Z is expressed as:

$$Z = \frac{Z_1 Z'}{Z_1 + Z'} \tag{5}$$

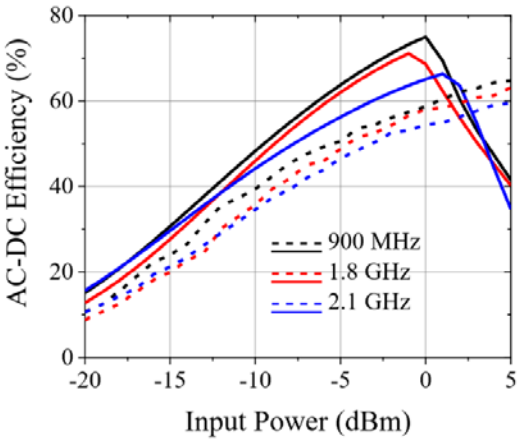

Figure 11. Simulated and measured AC-DC efficiency of the three rectifiers, solid lines are simulated results, dashed lines are measurement results.

The value of Z_1 is calculated so that $Z = 50\,\Omega$ at 900 MHz. Since Z_1 can be calculated after the length and width of the stub, and the frequency using Equation (1), the suitable size of the stub is obtained.

Finally, three rectifiers are DC-combined, and their common load are swept to obtain the optimal load, which is 2.7 kΩ.

The efficiency of the rectifiers is shown in Fig. 11. Due to fabrication error, especially during the welding step, the efficiency is somewhat different from simulation. However, the efficiency still reaches as high as 65% at 5 dBm input power for the 900 MHz rectifier, 63% and 60% at 5 dBm for the 1.8 GHz and 2.1 GHz rectifiers. At low input power, namely −10 dBm, the efficiencies are respectively 40%, 36%, and 35% for the three rectifiers. These performances are comparable to most of the previously proposed multiband rectifiers [6–9] while the advantage in simplicity is visible.

3. TRIPLE-BAND RECTENNA EXPERIMENT

The antenna, triplexer, and rectifiers are connected to form a complete triple-band rectenna, as shown in Fig. 12. The rectenna is put under test. Incident wave is excited from a Keysight N5182B MXG signal generator. A reference antenna, with the gain of 8 dBi at 900 MHz, 11 dBi at 1.8 GHz, and 12 dBi at 2.1 GHz, is used to transmit the excited wave. The rectenna is placed 1.5 meters away from the reference antenna. The incident power at each frequency $P_{in}(f)$ is calculated as follows:

$$P_{in}(f) = \frac{P(f)G(f)}{4\pi d^2 A(f)} \tag{6}$$

where $P(f)$, $G(f)$, and $A(f)$ are the excited power, reference antenna's gain, and receiving antenna's effective aperture at the corresponding frequency, respectively; $d = 1.5$ m is the distance between two antennas. The RF-DC efficiency $\eta_{\text{RF-DC}}$ is calculated after the incident power, the load R, and the output voltage V as follows:

$$\eta_{\text{RF-DC}} = \frac{V^2/R}{\left(P_{in}\left(900\,\text{MHz}\right) + P_{in}\left(1.8\,\text{GHz}\right) + P_{in}\left(2.1\,\text{GHz}\right)\right)} \times 100\% \tag{7}$$

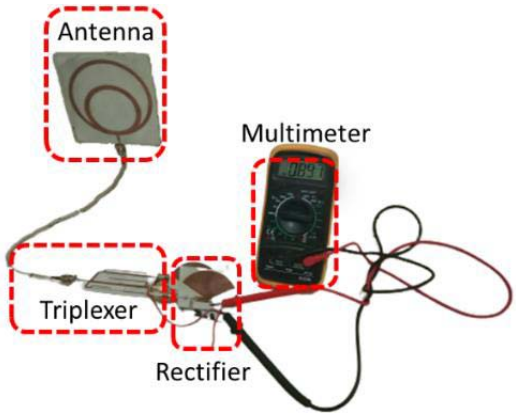

Figure 12. The complete triplexer-based triple-band rectenna.

The antenna is tested both monotonically and triple-tonically, with both sinusoidal signal and non-sinusoidal modulated signal, corresponding to ambient RF sources. The measurement results are displayed in Fig. 13. As shown in Fig. 13(a), under 5 dBm sinusoidal incidence, the efficiency reaches up to 60%, 48%, 50% at 900 MHz, 1.8 GHz, and 2.1 GHz, respectively. The triple-tone efficiency is higher, reaching up to 68%. For lower incident power, namely −10 dBm, the monotone efficiency is respectively 37%, 28%, 30% at 900 MHz, 1.8 GHz, and 2.1 GHz. Meanwhile, the triple-tone efficiency is 40%. For modulated signal, due to limited facility, we cannot perform triple-tonic measurement. The efficiency is somewhat lower, reaching respectively 33%, 26%, 28% at 900 MHz, 1.8 GHz, and 2.1 GHz for −10 dBm input, as shown in Fig. 13(b).

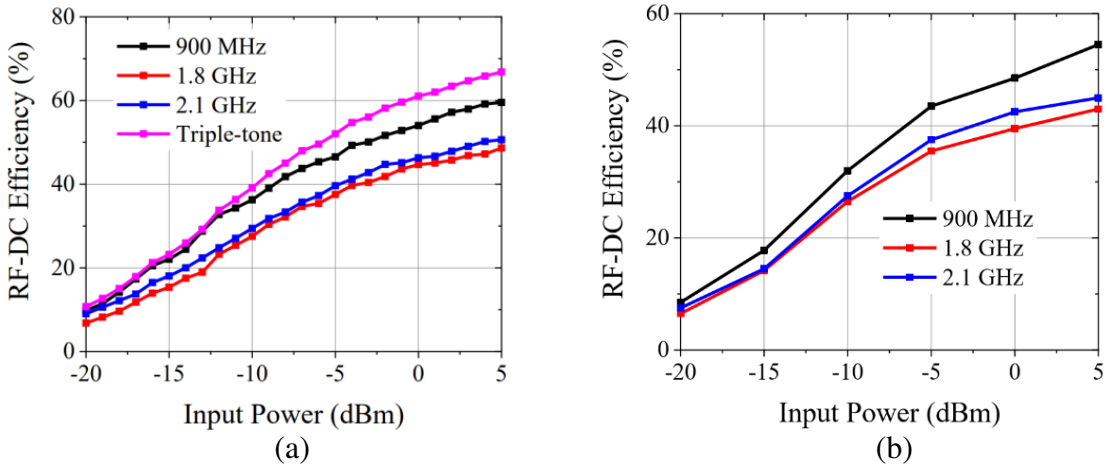

Figure 13. Measured RF-DC efficiency with (a) sinusoidal wave and (b) modulated wave.

Table 2 shows the comparison between the rectenna of this work and several related works. In general, the performances are comparable, and this rectenna is even slightly better in efficiency. The single-tone efficiency at 900 MHz is lower than that of the rectenna in [7], probably because rectenna employs only one diode instead of two. However, this design is significantly simpler thank to the monoband rectifiers.

In addition, because the antenna, triplexer, and rectifiers are fabricated on the same type of substrate, they can be integrated into a monolithic rectenna. In such a case, as the SMA connectors are removed, the conversion efficiency can be improved.

For input power as low as −10 dBm, the rectenna harvests up to 40 μW DC power. This amount of power is, unfortunately, still insufficient to fully supply a wireless sensor in full active mode. However, several wireless sensors only consume several nanowatts in sleep mode and several microwatts in some other limited actions, and can be supplied by this rectenna. For higher input power, such as 5 dBm, the amount of harvested power is 2.2 mW. However, such a high input is rarely found in the ambience, unless the rectenna is placed very close to the wave sources such as base transceiver towers.

Table 2. A comparison between the rectenna of this work and related works.

Work	Frequency (GHz)	Efficiency at −10 dBm (%)	Antenna	Configuration
[6]	2.45, 3.6	26, 15	Composite Right-left handed metamaterial antenna	Dual-band rectifier
[7]	0.9, 1.8, 2.1	41, 30, 25	Dual-port patch antenna with auxiliary patch director	Multiband rectifier
[22]	2.45, 5.5	20, 3	Slotted patch antenna	Dual-band rectifier
[23]	1.8, 2.1	28, 36	Slotted monopole antenna	Dual-band rectifier
[24]	0.866, 1.841, 1.957	20, 13, 13	Slotted patch antenna	Multiband rectifier
This work	0.9, 1.8, 2.1	33, 26, 28 (single-tone) 40% (triple-tone)	Multiple-ring monopole	Triplexer and monoband rectifiers

4. CONCLUSION

In conclusion, in this paper, we have designed and examined a triple-band rectenna for ambient RF energy harvesting. The rectenna, standing out by simplicity, consists of a multiband antenna, a triplexer, and three monoband rectifiers. The antenna is made by superposing two different rings to create multiple resonant frequencies, and more bands can be made by superposing more rings into the structure. The antenna is multi-directional, yielding gains of 2.5 dBi, 4.5 dBi, and 4 dBi at 900 MHz, 1.8 GHz, and 2.1 GHz, respectively. The triplexer is formed by conventional quarter-wavelength open stubs and can be easily upgraded into a quadruplexer or more, by employing more stubs. The triplexing efficiency is higher than 75%, better than most earlier works. The rectenna is therefore easy to modify to incorporate more harvested bands, further increasing the amount of harvested power. The final RF-DC efficiency of the rectenna is 40% at -10 dBm input power for triple-tone incidence. This performance is better than or comparable to several related works, but the simplicity in rectifier design and the expandability are the key advantages, making it suitable for practical application. With such efficiency, at low incident power, the harvested power is enough for several IoT devices at sleep mode or some limited actions, but insufficient for fully active modes, unless the rectenna is placed very close to the RF sources. Another problem is the size of the multiplexer, which increases steadily if more stubs (more frequency bands) are incorporated. This problem requires further study on miniaturization and will be addressed in future works.

ACKNOWLEDGMENT

This research is funded by the Ministry of Education and Training (MOET) under grant number B2020-BKA-11.

REFERENCES

1. Vullers, R., R. Schaijk, H. Visser, J. Penders, and C. Hoof, "Energy harvesting for autonomous wireless sensor networks," *IEEE Solid-State Circuits Mag.*, Vol. 2, No. 2, 29–38, 2010.
2. Nguyen, N., Q. C. Nguyen, and M. T. Le, "A novel autonomous wireless sensor node for IoT applications," *TELKOMNIKA Telecommun. Comput. Electron. Control*, Vol. 17, No. 5, 2389, Oct. 2019.
3. Nguyen, T. H., et al., "Smart shoe based on battery-free Bluetooth low energy sensor," *Industrial Networks and Intelligent Systems*, N.-S. Vo, V.-P. Hoang, and Q.-T. Vien, Eds., Vol. 379, 156–166, Springer International Publishing, Cham, 2021.
4. Cansiz. M., D. Altinel, and G. K. Kurt, "Efficiency in RF energy harvesting systems: A comprehensive review," *Energy*, Vol. 174, 292–309, May 2019.
5. Pinuela, M., P. D. Mitcheson, and S. Lucyszyn, "Ambient RF energy harvesting in urban and semi-urban environments," *IEEE Trans. Microw. Theory Tech.*, Vol. 61, No. 7, 2715–2726, Jul. 2013.
6. Chandrasekaran, K. T., K. Agarwal, Nasimuddin, A. Alphones, R. Mittra, and M. F. Karim, "Compact dual-band metamaterial-based high-efficiency rectenna: An application for ambient electromagnetic energy harvesting," *IEEE Antennas Propag. Mag.*, Vol. 62, No. 3, 18–29, Jun. 2020.
7. Shen, S., C.-Y. Chiu, and R. D. Murch, "A dual-port triple-band L-probe microstrip patch rectenna for ambient RF energy harvesting," *IEEE Antennas Wirel. Propag. Lett.*, Vol. 16, 3071–3074, 2017.
8. Mansour, M. M. and H. Kanaya, "Compact and broadband RF rectifier with 1.5 octave bandwidth based on a simple pair of L-section matching network," *IEEE Microw. Wirel. Compon. Lett.*, Vol. 28, No. 4, 335–337, Apr. 2018.
9. Daskalakis, S. N., A. Georgiadis, A. Collado, and M. M. Tentzeris, "An UHF rectifier with 100% bandwidth based on a ladder LC impedance matching network," *2017 12th European Microwave Integrated Circuits Conference (EuMIC)*, 411–414, Nuremberg, Oct. 2017.
10. Gorur, A. K. and C. Karpuz, "A novel microstrip triplexer based on meandered loop resonators," *2017 IEEE Asia Pacific Microwave Conference (APMC)*, 1242–1245, Kuala Lumpar, Nov. 2017.

11. Tang, C.-W. and C.-T. Tseng, "Design of a packaged microstrip triplexer with star-junction topology," *2012 42nd European Microwave Conference*, 459–462, Amsterdam, Oct. 2012.
12. Chen, C.-F., T.-Y. Huang, T.-M. Shen, and R.-B. Wu, "A miniaturized microstrip common resonator triplexer without extra matching network," *2006 Asia-Pacific Microwave Conference*, 1439–1442, Yokohama, Japan, Dec. 2006.
13. Elwi, T. A., Z. A. Abdul Hassain, and O. A. Tawfeeq, "Hilbert metamaterial printed antenna based on organic substrates for energy harvesting," *IET Microw. Antennas Propag.*, Vol. 13, No. 12, 2185–2192, Oct. 2019.
14. Elwi, T. A. and S. G. Abdulqader, "Further investigation on solant–rectenna-based flexible Hilbert-shaped metamaterials," *IET Nanodielectrics*, Vol. 3, No. 3, 88–93, Sep. 2020.
15. Elwi, T. A. and A. M. Al-Saegh, "Further realization of a flexible metamaterial-based antenna on indium nickel oxide polymerized palm fiber substrates for RF energy harvesting," *Int. J. Microw. Wirel. Technol.*, Vol. 13, No. 1, 67–75, Feb. 2021.
16. Elwi, T. A., "Novel UWB printed metamaterial microstrip antenna based organic substrates for RF-energy harvesting applications," *AEU — Int. J. Electron. Commun.*, Vol. 101, 44–53, Mar. 2019.
17. Al-Dulaimi, Z., T. A. Elwi, D. C. Atilla, and C. Aydin, "Design of fractal based monopole antenna array with ultra-mutual coupling reduction for MIMO applications," *2018 18th Mediterranean Microwave Symposium (MMS)*, 39–42, Istanbul, Oct. 2018.
18. Pandey, R., A. K. Shankhwar, and A. Singh, "Design, analysis, and optimization of dual side printed multiband antenna for RF energy harvesting applications," *Progress In Electromagnetics Research C*, Vol. 102, 79–91, 2020.
19. Deng, P.-H., M.-I. Lai, S.-K. Jeng, and C. H. Chen, "Design of matching circuits for microstrip triplexers based on stepped-impedance resonators," *IEEE Trans. Microw. Theory Tech.*, Vol. 54, No. 12, 4185–4192, Dec. 2006.
20. El-Tokhy, A., R. Wu, and Y. Wang, "Microstrip triplexer using a common triple-mode resonator," *Microw. Opt. Technol. Lett.*, Vol. 60, No. 7, 1815–1820, Jul. 2018.
21. Hemour, S., et al., "Towards low-power high-efficiency RF and microwave energy harvesting," *IEEE Trans. Microw. Theory Tech.*, Vol. 62, No. 4, 965–976, Apr. 2014.
22. Mattsson, M., C. I. Kolitsidas, and B. L. G. Jonsson, "Dual-band dual-polarized full-wave rectenna based on differential field sampling," *IEEE Antennas Wirel. Propag. Lett.*, Vol. 17, No. 6, 956–959, Jun. 2018.
23. Khemar, A., A. Kacha, H. Takhedmit, and G. Abib, "Design and experiments of a dual-band rectenna for ambient RF energy harvesting in urban environments," *IET Microw. Antennas Propag.*, Vol. 12, No. 1, 49–55, Jan. 2018.
24. Boursianis, A. D., et al., "Triple-band single-layer rectenna for outdoor RF energy harvesting applications," *Sensors*, Vol. 21, No. 10, 3460, May 2021.
25. Balanis, C. A., *Antenna Theory: Analysis and Design*, 4th Edition, Wiley, Hoboken, New Jersey, 2016.